Perilipin 1 (Plin1) deficiency promotes inflammatory responses in lean adipose tissue through lipid dysregulation

Received for publication, April 18, 2018, and in revised form, July 18, 2018 Published, Papers in Press, July 24, 2018, DOI 10.1074/jbc.RA118.003541

Jee Hyung Sohn[‡1], Yun Kyung Lee[‡], Ji Seul Han[‡1], Yong Geun Jeon[‡1], Jong In Kim[‡1], Sung Sik Choe[‡], Su Jung Kim[§], Hyun Ju Yoo[§], and Jae Bum Kim[‡2]

From the [‡]National Creative Research Initiatives Center for Adipose Tissue Remodeling, Institute of Molecular Biology and Genetics, Department of Biological Sciences, Seoul National University, Seoul KS013 and the [§]Department of Convergence Medicine, Asan Institute for Life Sciences, Asan Medical Center, University of Ulsan College of Medicine, Seoul KS013, South Korea

Edited by George M. Carman

Lipid droplets are specialized cellular organelles that contain neutral lipid metabolites and play dynamic roles in energy homeostasis. Perilipin 1 (*Plin1*), one of the major lipid droplet-binding proteins, is highly expressed in adipocytes. In mice, *Plin1* deficiency impairs peripheral insulin sensitivity, accompanied with reduced fat mass. However, the mechanisms underlying insulin resistance in lean *Plin1* knockout (*Plin1*$^{-/-}$) mice are largely unknown. The current study demonstrates that *Plin1* deficiency promotes inflammatory responses and lipolysis in adipose tissue, resulting in insulin resistance. M1-type adipose tissue macrophages (ATMs) were higher in *Plin1*$^{-/-}$ than in *Plin1*$^{+/+}$ mice on normal chow diet. Moreover, using lipidomics analysis, we discovered that *Plin1*$^{-/-}$ adipocytes promoted secretion of pro-inflammatory lipid metabolites such as prostaglandins, which potentiated monocyte migration. In lean *Plin1*$^{-/-}$ mice, insulin resistance was relieved by macrophage depletion with clodronate, implying that elevated pro-inflammatory ATMs might be attributable for insulin resistance under *Plin1* deficiency. Together, these data suggest that *Plin1* is required to restrain fat loss and pro-inflammatory responses in adipose tissue by reducing futile lipolysis to maintain metabolic homeostasis.

Chronic, low-grade inflammation is a major factor in the pathogenesis of insulin resistance (1, 2). Macrophages play an important role in the modulation of inflammation through their capacity to secrete a variety of chemokines and cytokines. Monocyte-originated macrophages polarize to classically activated macrophages (M1) or alternatively activated macrophages (M2) in certain tissue niches and upon environmental stimuli (3). In fact, alteration of adipose tissue macrophages (ATMs)[3] contributes to elevated adipose tissue inflammation in obesity (4, 5). In obesity, macrophages are recruited into adipose tissue and show pro-inflammatory properties compared with resident ATMs (6). Thus, M1-type macrophages, which secrete pro-inflammatory cytokines such as tumor necrosis factor (TNF) α, interleukin (IL)-6, and monocyte chemoattractant protein (MCP)-1, are the predominant ATM population in obese adipose tissue (4, 5, 7). Adipose tissue inflammation is also observed in lipodystrophic and cachectic subjects, accompanied with fat loss (8–12). ATM infiltration has been reported in several lipodystrophic animal models and human patients (8–10). Moreover, cachexia is associated with elevated pro-inflammatory gene expression, macrophage infiltration, and fibrosis in adipose tissue of cancer patients (11, 12).

Lipid dysregulation is closely related to various pathophysiologies, such as rheumatoid arthritis, multiple sclerosis, and obesity-induced insulin resistance (13, 14). Although lipid metabolites have been considered as simple energy sources, recent findings have revealed that lipid metabolites can also act as signaling molecules for immune responses (15, 16). In obesity, elevated fatty acids are a potential trigger for macrophage activation (17). For instance, saturated fatty acids stimulate Toll-like receptor (TLR) 4 in ATMs, resulting in the activation of inflammatory signaling cascades mediated by NF-κB (17). Also, leukotriene B_4 promotes chemotactic activity of macrophages, which contribute to whole-body insulin resistance (18).

Lipid droplets are metabolically dynamic cellular organelles specialized in storing free fatty acids (FFAs) and sterols in the form of triglycerides (TG) and cholesterol esters, respectively (19, 20). This sequestration of lipid metabolites into lipid droplets contributes to relieve from toxic effects the excess FFAs or sterols that can lead to insulin resistance and inflammation (21, 22). Perilipin 1 (*Plin1*), the most abundant lipid droplet coat protein in adipocytes, is required for optimal lipid homeostasis

This work was supported by a National Research Foundation of Korea (NRF) grant funded by the South Korea government, Ministry of Science, ICT, and Future Planning number 2011–0018312. The authors declare that they have no conflicts of interest with the contents of this article. The content is solely the responsibility of the authors and does not necessarily represent the official views of the National Institutes of Health.

This article contains Table S1.

[1] Supported by the Brain Korea 21 program.

[2] To whom correspondence should be addressed: Dept. of Biological Sciences, National Creative Research Initiatives Center for Adipose Tissue Remodeling, Institute of Molecular Biology and Genetics, Seoul National University, San 56-1, Shillim-dong, Gwanak-gu, Seoul 151-742, South Korea. Tel.: 82-2-880-5852; Fax: 82-2-878-5852; E-mail: jaebkim@snu.ac.kr.

[3] The abbreviations used are: ATM, adipose tissue macrophage; TG, triglyceride; TNF, tumor necrosis factor; MCP, monocyte chemoattractant protein; FFA, free fatty acid; HSL, hormone-sensitive lipase; CGI-58, comparative gene identification 58; ATGL, adipose triglyceride lipase; NCD, normal chow diet; PG, prostaglandin; WAT, white adipose tissue; SVC, stromal vascular cell; CM, conditioned medium; AA, arachidonic acid; COX, cyclooxygenase; GTT, glucose tolerance test; ITT, insulin tolerance test; PVAT, perivascular adipose tissue; DMEM, Dulbecco's modified Eagle's medium; FBS, fetal bovine serum; qRT, quantitative reverse transcription; ANOVA, analysis of variance; iWAT, inguinal white adipose tissue; eWAT, epididymal white adipose tissue.

(23). In the basal state, PLIN1 encloses lipid droplets and inhibits its lipolysis in adipocytes (24). On the contrary, catecholamine promotes lipolysis by inducing the translocation of hormone-sensitive lipase (HSL) onto lipid droplets (25, 26). Although PLIN1 binds to comparative gene identification-58 (CGI-58), a coactivator of adipose triglyceride lipase (ATGL) in the basal state, PLIN1 liberates CGI-58 to induce lipolysis upon protein kinase A activation during the stimulated state (27). It has been reported that *Plin1*$^{-/-}$ mice are lean and exhibit glucose intolerance and insulin resistance in the absence of any metabolic stress (24). However, the molecular mechanisms of insulin resistance in normal chow diet (NCD)-fed lean *Plin1*$^{-/-}$ mice have not been fully elucidated.

In this study, we investigated NCD-fed lean *Plin1*$^{-/-}$ mice to understand the molecular mechanisms underlying insulin resistance under *Plin1* deficiency. We demonstrate that *Plin1* deficiency stimulates pro-inflammatory responses in adipose tissue by secreting pro-inflammatory lipid metabolites, which exacerbate adipose tissue inflammation. Using lipidomics analysis, we found that elevated prostaglandins (PGs) from *Plin1*$^{-/-}$ adipocytes potentiated monocyte migration. In addition, depletion of ATMs with clodronate alleviated insulin resistance in *Plin1*-deficient mice, implying that an increase in pro-inflammatory ATMs is one of the major inducers for insulin resistance in *Plin1*$^{-/-}$ mice. Together, these data suggest that *Plin1* is an important protective regulator against adipose tissue inflammation and insulin resistance by restricting futile lipolysis.

Results

CD11b-positive cells are increased in adipose tissue of Plin1$^{-/-}$ *mice*

Plin1 expression is decreased in adipose tissue from insulin-resistant animals (28). Consistent with this finding, the levels of *Plin1* mRNA and protein were lower in adipocytes from *db*/*db* mice and adipose tissue from high fat diet-fed mice than in those from *db*/+ mice and NCD-fed mice (Fig. 1, *A* and *B*). Nonetheless, it remained unclear how *Plin1* deficiency could influence whole-body energy homeostasis. To address this, we investigated various physiological parameters in *Plin1*$^{-/-}$ mice in C57BL/6J background (24) compared with littermate WT mice (*Plin1*$^{+/+}$). Under NCD-fed conditions, body weights were not significantly different between *Plin1*$^{+/+}$ and *Plin1*$^{-/-}$ mice (Fig. 1*C*). However, inguinal white adipose tissue (iWAT) and epididymal white adipose tissue (eWAT) weights, but neither liver nor brown adipose tissue weights, were lower in *Plin1*$^{-/-}$ than in *Plin1*$^{+/+}$ mice (Fig. 1*D*). In addition, serum TG and FFAs, but not cholesterol, were slightly higher in *Plin1*$^{-/-}$ than in *Plin1*$^{+/+}$ mice (Fig. 1, *E–G*). Hematoxylin and eosin (H&E) staining of eWAT revealed that lipid droplets were smaller in size in *Plin1*$^{-/-}$ than in *Plin1*$^{+/+}$ mice (Fig. 1*H*). Interestingly, the intensity of CD11b staining in eWAT of NCD-fed *Plin1*$^{-/-}$ mice was markedly increased (Fig. 1*I*), suggesting that *Plin1* deficiency might be associated with adipose tissue inflammation in lean animals.

Plin1 deficiency induces macrophage accumulation and adipose tissue inflammation

In adipose tissue, macrophages are one of the abundant cell types and determine the degree of fat tissue inflammation (4, 5). To investigate whether *Plin1* deficiency might be related with adipose tissue inflammation, we examined inflammatory gene expression and macrophage accumulation in eWAT from NCD-fed *Plin1*$^{+/+}$ and *Plin1*$^{-/-}$ mice. As shown in Fig. 2*A*, *Plin1*-deficient eWAT had markedly increased mRNA levels of the pro-inflammatory cytokine genes including *Mcp-1* and *Tnfα* as well as of the macrophage marker genes such as *F4/80* and *Cd11c*. In addition, serum levels of pro-inflammatory cytokines such as MCP-1 and TNFα were induced in *Plin1*$^{-/-}$ mice (Fig. 2*B*). In eWAT of *Plin1*$^{-/-}$ mice, CD11b^{+} and CD11c^{+} cells were increased (Fig. 2*C*). Also, *Plin1* deficiency elevated the percentages of F4/80^{+}CD11b^{+} (macrophages) and F4/80^{+}CD11b^{+}CD11c^{+} cells (M1-type macrophages) among stromal vascular cells (SVCs) from eWAT (Fig. 2, *D* and *E*). Total numbers of F4/80^{+}CD11b^{+} and F4/80^{+}CD11b^{+} CD11c^{+} cells (Fig. 2, *F* and *G*) were higher in eWAT of *Plin1*$^{-/-}$ than in that of *Plin1*$^{+/+}$ mice. Moreover, the percentage of M1-type CD11c^{+} cells in F4/80^{+}CD11b^{+} macrophages was higher in *Plin1*$^{-/-}$ than in *Plin1*$^{+/+}$ mice (Fig. 2*H*), whereas the fraction of M2-type CD206^{+} macrophages in F4/80^{+}CD11b^{+} cells was lower in *Plin1*$^{-/-}$ mice (Fig. 2*I*). Collectively, these results suggested that *Plin1* might play certain roles in the regulation of adipose tissue inflammation as well as ATM recruitment.

Plin1-deficient adipocytes stimulate monocyte migration and pro-inflammatory cytokine expression in macrophages

In adipose tissue, infiltration of immune cells including monocytes or macrophages and increased pro-inflammatory responses in macrophages are prominent in insulin-resistant animals (29, 30). To determine whether *Plin1* deficiency might be involved in the regulation of monocyte/macrophage migration, conditioned media (CM) obtained from *ex vivo* cultured eWAT of *Plin1*$^{-/-}$ and *Plin1*$^{+/+}$ mice were incubated with THP-1 monocytes or peritoneal macrophages (Fig. 3*A*). As shown in Fig. 3, *B* and *C*, the degrees of THP-1 and macrophage migration were higher in CM from *Plin1*$^{-/-}$ eWAT than in CM from *Plin1*$^{+/+}$ eWAT. Similarly, stimulatory effects were observed when CM were collected from primary *Plin1*$^{-/-}$ adipocytes in monocyte migration assays (Fig. 3, *A* and *D*). Next, we used a Transwell co-culture system to test whether macrophage gene expression might be affected by *Plin1* deficiency in eWAT or adipocytes (Fig. 3*E*). Relative mRNA levels of the pro-inflammatory response genes including *Il-6*, *iNOS*, and *Il-1β* were stimulated in macrophages when they were indirectly co-cultured with eWAT from *Plin1*$^{-/-}$ mice (Fig. 3*F*). Primary adipocytes from *Plin1*$^{-/-}$ mice also promoted the mRNA levels of these factors in macrophages (Fig. 3*G*). However, *Plin1*$^{-/-}$ macrophages and *Plin1*$^{+/+}$ macrophages did not show any difference in inflammatory gene expression (Fig. 3*H*). These results indicated that *Plin1* would act as a protective factor against adipose tissue inflammation, at least in part by inhibiting the secretion of certain signaling molecule(s) that

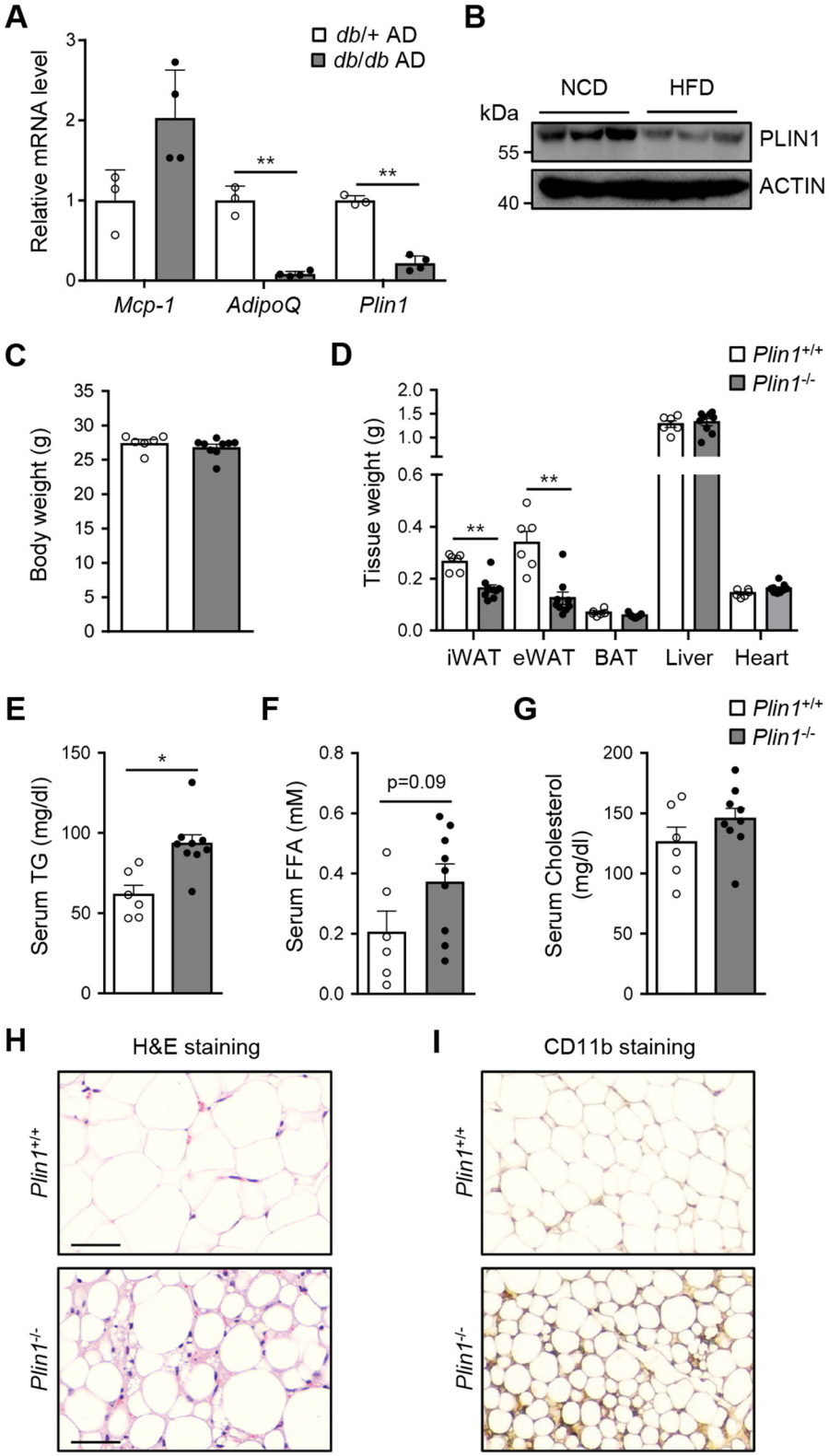

Figure 1. *Plin1*$^{-/-}$ mice show hypotrophy of adipose tissue with elevated macrophages. *A,* expression levels of *Plin1* mRNA in adipocytes (AD) of *db*/+ and *db*/*db* mice were determined by qRT-PCR. **, $p < 0.01$ *versus db*/+ group by Student's *t* test. *B,* C57BL/6J mice were fed NCD or high fat diet (*HFD*) for 20 weeks. eWAT were obtained and subjected to immunoblot analysis using anti-PLIN1 and anti-ACTIN antibodies. *C–G,* body weight (*C*), the weights of various tissues (*D*), and the levels of serum TG (*E*), serum FFAs (*F*), and serum cholesterol (*G*) from *Plin1*$^{+/+}$ and *Plin1*$^{-/-}$ mice were measured. *H,* adipocyte morphology of eWAT from *Plin1*$^{-/-}$ and *Plin1*$^{+/+}$ mice was assessed by hematoxylin and eosin (H&E) staining. *Scale bars*, 50 μm. *I,* myeloid cells were detected in eWAT from *Plin1*$^{+/+}$ and *Plin1*$^{-/-}$ mice by diaminobenzidine staining with an anti-mouse CD11b antibody. ×100 magnification. All data represent the mean ± S.E. *, $p < 0.05$; **, $p < 0.01$ *versus Plin1*$^{+/+}$ group by Student's *t* test.

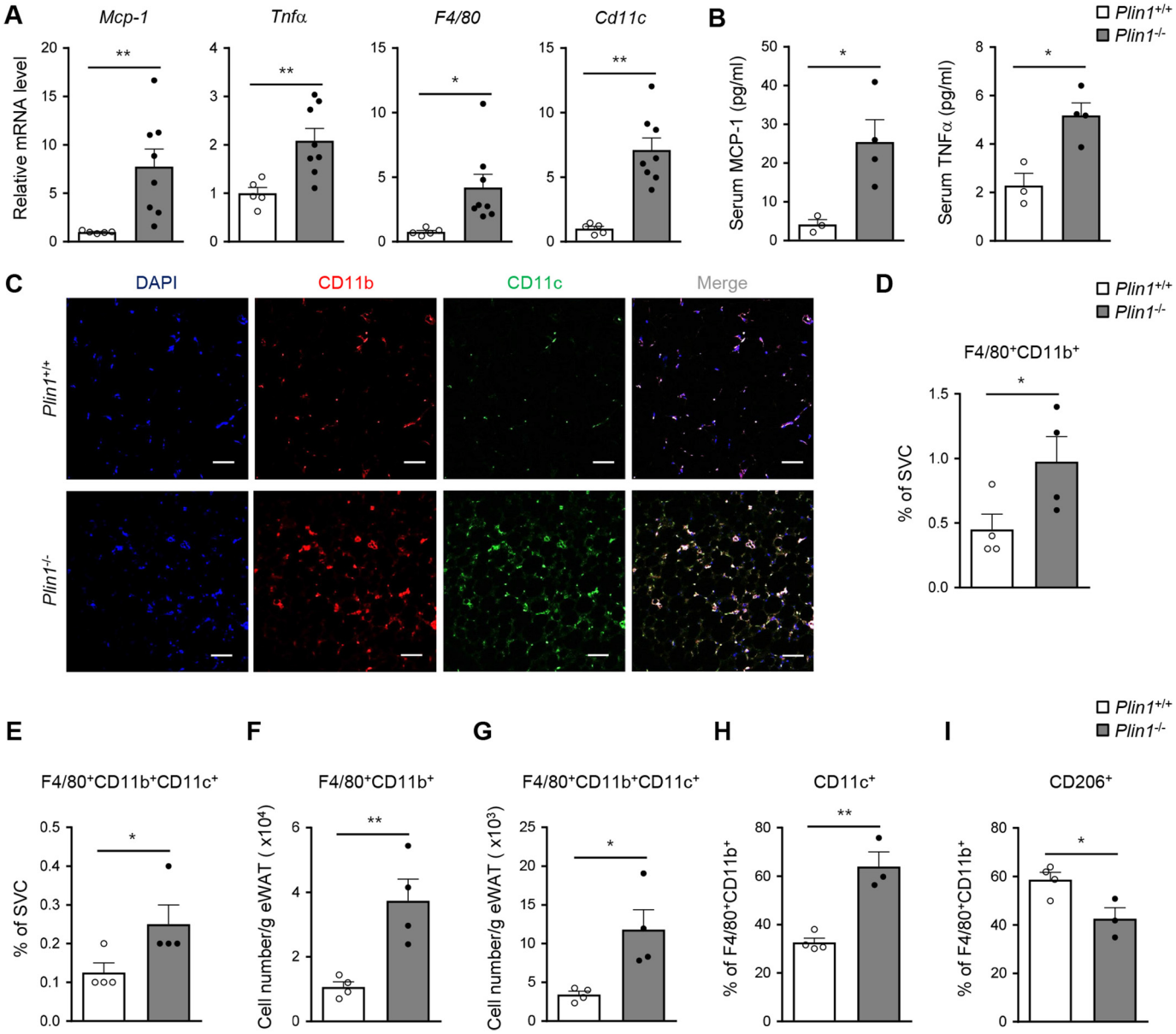

Figure 2. Adipose tissue inflammation is enhanced in *Plin1*$^{-/-}$ mice. *A,* relative mRNA levels of inflammatory cytokine genes (*Mcp-1* and *Tnfα*) and macrophage markers (*F4/80* and *Cd11c*) were measured in eWAT by qRT-PCR. *B,* serum levels of MCP-1 and TNFα were assessed by ELISA. *C,* macrophage accumulation was detected in eWAT from *Plin1*$^{+/+}$ and *Plin1*$^{-/-}$ mice by immunohistochemistry analysis of the nuclei (*blue*), CD11b (*red*), and CD11c (*green*). *Scale bars*, 50 μm. *D–I*, macrophage accumulation was measured in eWAT by flow cytometric analysis. The percentages of F4/80$^+$CD11b$^+$ (*D*) and F4/80$^+$CD11b$^+$CD11c$^+$ (*E*) cells in the SVCs of eWAT are shown in the graphs. Total numbers of F4/80$^+$CD11b$^+$ (*F*) and F4/80$^+$CD11b$^+$CD11c$^+$ (*G*) cells in SVCs/g of eWAT were determined. Percentages of CD11c$^+$ (*H*) and CD206$^+$ (*I*) cells in the F4/80$^+$CD11b$^+$ cells were measured. All data represent the mean ± S.E. *, $p < 0.05$; **, $p < 0.01$ *versus Plin1*$^{+/+}$ group by Student's *t* test. All qRT-PCR data were normalized to the mRNA level of *cyclophilin*.

promote the expression of pro-inflammatory cytokines and monocyte migration.

In Plin1-deficient adipocytes, enhanced lipolysis promotes monocyte migration

In adipocytes, *Plin1* is a key player to modulate lipolysis (24, 27). To determine whether the inhibitory effect of *Plin1* on lipolysis might be associated with monocyte migration, we first examined the effect of *Plin1* deficiency on the release of lipolytic metabolites in culture media. As expected, *Plin1*$^{-/-}$ adipocytes secreted higher amounts of glycerol and FFAs than *Plin1*$^{+/+}$ adipocytes (Fig. 4, *A* and *B*). On the other hand, *Plin1*-deficient adipocytes showed little or no effect on MCP-1 secretion (Fig. 4*C*). Moreover, to examine whether increased monocyte migration upon *Plin1* deficiency depends on secretory proteins from adipocytes, CM from SVC-derived adipocytes was subjected to heat inactivation (31). Heat-inactivated CM from *Plin1*$^{-/-}$ adipocytes did not significantly alter the degree of monocyte migration compared with CM from *Plin1*$^{-/-}$ adipocytes (Fig. 4*D*). These data imply that increased monocyte migration upon *Plin1* deficiency might not be associated with secreted chemokines from adipocytes.

To investigate whether enhanced lipolysis in *Plin1*-deficient adipocytes might be attributable to monocyte migration, two key lipases, *Atgl* and *Hsl*, were knocked down via siRNA in SVC-derived adipocytes (Fig. 4, *E* and *F*). Basal lipolysis was

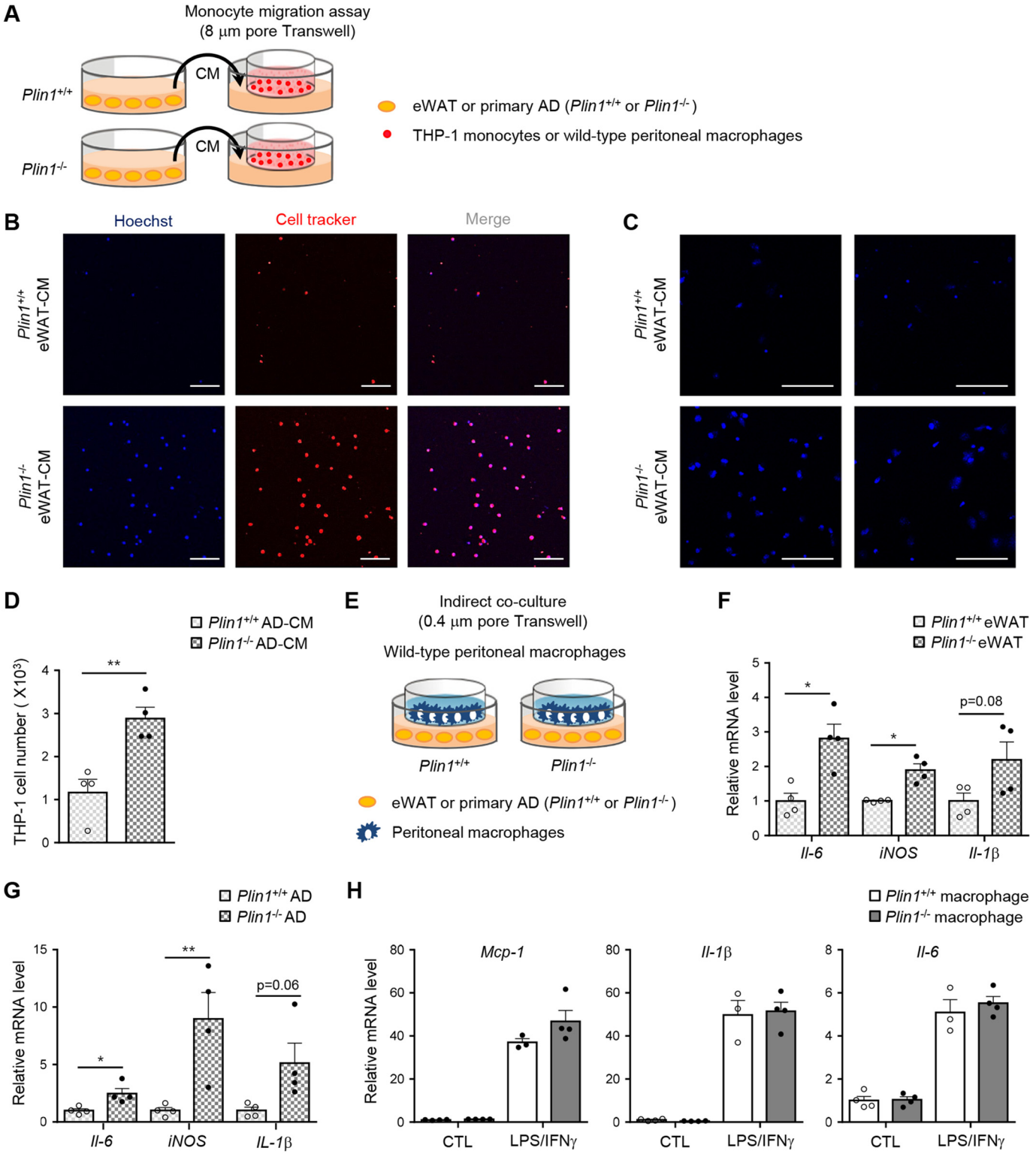

Figure 3. *Plin1*$^{-/-}$ adipocytes enhance monocyte migration and macrophage activation. *A*, eWAT or primary adipocytes from *Plin1*$^{+/+}$ and *Plin1*$^{-/-}$ mice were incubated with culture medium for 48 h. Collected CM was tested for Transwell culture. THP-1 monocytes were prestained with CellTracker (*red*), and incubated for 6 h in Transwell plates (8 μm pore size) with CM. Peritoneal macrophages were incubated with CM for 6 h, and stained with Hoechst (*blue*). Migrated monocytes (*B*) or macrophages (*C*) upon incubation with eWAT CM were assessed by confocal microscope. *Scale bars*, 100 μm. *D*, the number of migrated cells upon incubation with primary adipocytes CM was measured. *E*, peritoneal macrophages were co-cultured with chopped eWAT or primary adipocytes of *Plin1*$^{+/+}$ and *Plin1*$^{-/-}$ mice in Transwell plates (0.4 μm pore) for 48 h. Total RNA was isolated from peritoneal macrophages co-cultured with eWAT (*F*) or primary adipocytes (*G*) for determining the mRNA levels of *Il-6*, *iNOS*, and *Il-1β*. *H*, peritoneal macrophages were treated 17 h with LPS (5 ng/ml) and interferon (*IFN*) γ (100 units/ml) and subjected to qRT-PCR to determine the expression of the indicated inflammatory genes. All data represent the mean ± S.E. *, $p < 0.05$; **, $p < 0.01$ *versus* *Plin1*$^{+/+}$ group by Student's *t* test. All qRT-PCR data were normalized to the mRNA level of *cyclophilin*. AD, adipocytes.

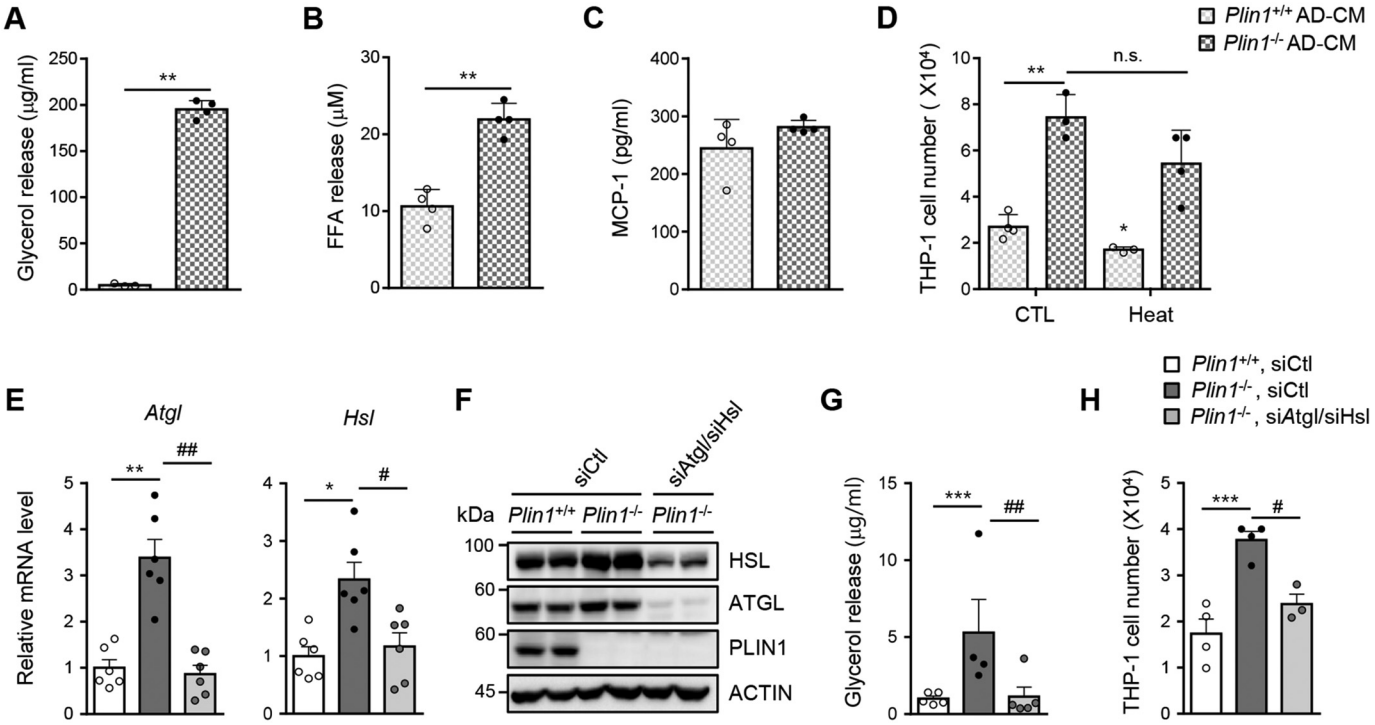

Figure 4. Suppression of enhanced lipolysis in *Plin1*$^{-/-}$ adipocytes alleviates monocyte migration. The levels of glycerol (*A*), FFAs (*B*), and MCP-1 (*C*) released from *Plin1*$^{+/+}$ or *Plin1*$^{-/-}$ primary adipocytes for 48 h were measured. **, $p < 0.01$ *versus Plin1*$^{+/+}$ group by Student's *t* test. *D,* CM were collected from SVC-derived adipocytes for 48 h and subjected to heat inactivation (70 °C, 10 min). The number of migrated cells upon incubation with each CM was measured. *, $p < 0.05$; **, $p < 0.01$ *versus Plin1*$^{+/+}$, CTL group by two-way ANOVA followed by Bonferroni's post hoc test. *E–H,* SVC-derived adipocytes were transfected with control siRNA (*siCtl*) or *Atgl*-specific siRNA (*siAtgl*) and *Hsl*-specific siRNA (*siHsl*). After 48 h, total RNA or protein was extracted and CM was collected from siRNA-transfected SVC-derived adipocytes. The mRNA levels of *Atgl* and *Hsl* were analyzed by qRT-PCR (*E*) and protein levels of ATGL and HSL were analyzed by Western blotting (*F*). The released glycerol (*G*) was measured. The number of migrated cells upon incubation with each CM was measured (*H*). *, $p < 0.05$; **, $p < 0.01$; ***, $p < 0.001$ *versus Plin1*$^{+/+}$, siCtl group; #, $p < 0.05$; ##, $p < 0.01$ *versus Plin1*$^{-/-}$, siCtl group by one-way ANOVA followed by Tukey's post hoc test. All data represent the mean ± S.E. All qRT-PCR data were normalized to the mRNA level of *cyclophilin*. *AD*, adipocytes.

markedly higher in *Plin1*$^{-/-}$ SVC-derived adipocytes than in *Plin1*$^{+/+}$ SVC-derived adipocytes (Fig. 4*G*). In *Plin1*$^{-/-}$ SVC-derived adipocytes, knockdown of *Atgl* and *Hsl* attenuated basal lipolysis (Fig. 4*G*). Intriguingly, the degree of monocyte migration was lower upon suppression of these lipases (Fig. 4*H*). Together, these results suggested that adipocyte *Plin1* would suppress adipose tissue inflammation through repressing basal lipolysis.

Elevated prostaglandins secreted from Plin1$^{-/-}$ *adipocytes potentiate monocyte migration*

Certain lipid metabolites, including leukotriene B_4, PGD_2, and PGE_2, promote monocyte/macrophage migration (18, 32). To identify potential secreted mediator(s) that can potentiate monocyte migration in adipose tissue of *Plin1*$^{-/-}$ mice, CM of adipocytes was subjected to lipidomic analysis by nontargeted LC-MS/MS (Table S1). The level of eicosanoids appeared to be higher in the CM of *Plin1*$^{-/-}$ adipocytes than in that of *Plin1*$^{+/+}$ adipocytes. We took a targeted lipidomics approach to determine the relative quantity of eicosanoids secreted from adipocytes (Fig. 5*A*). The level of PGE_2 was higher in the CM of *Plin1*$^{-/-}$ adipocytes than in that of *Plin1*$^{+/+}$ adipocytes (Fig. 5*B*).

Because cyclooxygenase (COX) isoenzymes produce PGs from arachidonic acid (AA) (Fig. 5*C*), intracellular AA was examined in adipocytes. As indicated in Fig. 5*D*, the level of AA appeared to be higher in *Plin1*$^{-/-}$ than in *Plin1*$^{+/+}$ adipocytes. Eukaryotic COX has two isoforms, *Cox1* and *Cox2*. Although *Cox1* is constitutively expressed and is involved in cellular homeostasis, *Cox2* is inducible and produces numerous PGs under pathophysiological conditions (33). To investigate whether *Plin1* deficiency might affect COX2 activity, we measured the enzymatic activity of COX from SVC-derived adipocytes. Although total COX activity was higher in *Plin1*$^{-/-}$ than in *Plin1*$^{+/+}$ adipocytes (Fig. 5*F*), suppression of *Cox2* via siRNA (Fig. 5*E*) down-regulated total COX activity in *Plin1*$^{-/-}$ adipocytes and suppressed the degree of monocyte migration (Fig. 5, *F* and *G*). Next, to examine the effect of elevated PGs on monocyte migration, SVC-derived adipocytes were treated with NS398, a COX2-selective inhibitor (Fig. 5*H*). As indicated in Fig. 5*I*, the degree of monocyte migration was mitigated by pharmacological inhibition of COX2 and restored by PGE_2 supplementation in CM. To further investigate how PGs might contribute to adipose tissue inflammation in *Plin1*$^{-/-}$ mice, we measured intracellular levels of PGE_2 and AA in eWAT from *Plin1*$^{+/+}$ and *Plin1*$^{-/-}$ mice. Although the levels of PGE_2 and AA in eWAT of *Plin1*$^{-/-}$ mice were increased (Fig. 5, *J* and *K*), the serum PGE_2 level was not altered upon *Plin1* deficiency (Fig. 5*L*). Moreover, in eWAT of NS398-treated *Plin1*$^{-/-}$ mice, pro-inflammatory gene expression profiles were significantly down-regulated compared with vehicle-treated *Plin1*$^{-/-}$ mice (Fig. 5*M*). These data proposed that increased PGs released from *Plin1*$^{-/-}$ adipocytes would stimulate monocyte migration.

Plin1$^{-/-}$ mice exhibit impaired insulin sensitivity via lipid dysregulation

To determine whether *Plin1* deficiency might alter systemic glucose homeostasis, the serum levels of glucose and insulin were measured. Compared with *Plin1*$^{+/+}$ mice, *Plin1*$^{-/-}$ mice exhibited higher fasting glucose and *ad libitum* insulin concentrations (Fig. 6, *A* and *B*). To investigate whether *Plin1* deficiency would indeed influence whole-body insulin sensitivity, we performed a glucose tolerance test (GTT) and insulin tolerance test (ITT). *Plin1*$^{-/-}$ mice were more glucose-intolerant and insulin-insensitive than *Plin1*$^{+/+}$ mice (Fig. 6, *C* and *D*). In accordance with these, the homeostatic model assessment-insulin resistance (HOMA-IR) index, a quantitative indicator of insulin resistance, was higher in *Plin1*$^{-/-}$ mice than *Plin1*$^{+/+}$

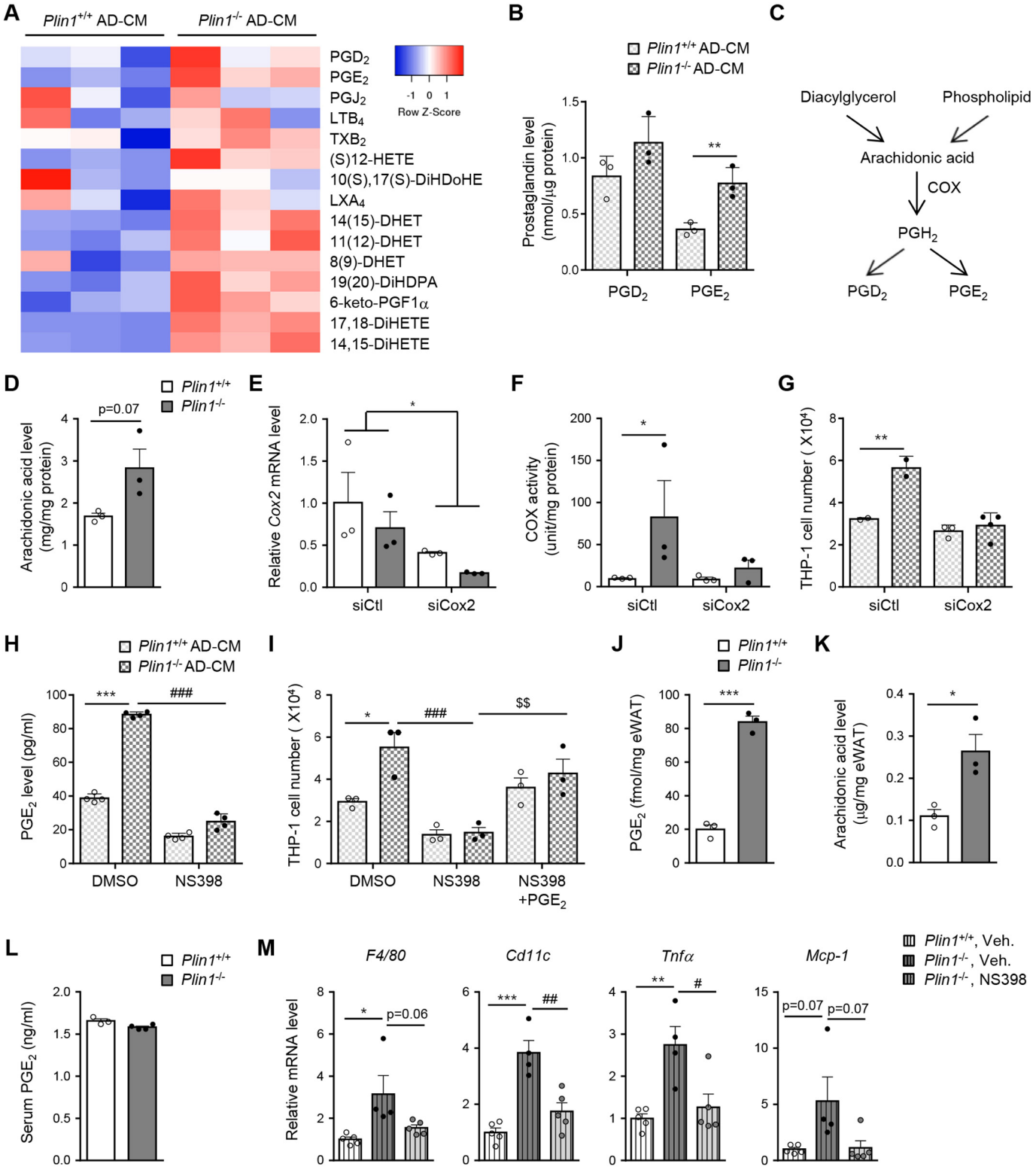

mice (Fig. 6*E*). Because NS398 administration reduced adipose tissue inflammation in *Plin1*$^{-/-}$ mice (Fig. 5), we further determined whether NS398 might alleviate insulin resistance in *Plin1*$^{-/-}$ mice. To address this, ITT was performed with vehicle- or NS398-treated *Plin1*$^{-/-}$ mice. As shown in Fig. 6*F*, NS398-treated *Plin1*$^{-/-}$ mice seemed to be less insulin intolerant. These data propose that abnormally up-regulated lipid metabolism would induce adipose tissue inflammation and insulin resistance in *Plin1*$^{-/-}$ mice.

We also examined whether *Plin1* deficiency might modulate insulin signaling cascades in metabolic organs. Insulin-stimulated AKT phosphorylation was lower in adipose tissue of *Plin1*$^{-/-}$ mice as well as in skeletal muscle of *Plin1*$^{-/-}$ mice (Fig. 6, *G* and *H*). In contrast, the level of AKT phosphorylation in the liver of *Plin1*$^{-/-}$ mice was not different from that in *Plin1*$^{+/+}$ mice (Fig. 6*I*). In addition, intracellular levels of TG and FFAs appeared to be increased in skeletal muscle of *Plin1*$^{-/-}$ mice but not in liver of *Plin1*$^{-/-}$ mice compared with *Plin1*$^{+/+}$ mice (Fig. 6, *J* and *K*). These results suggested that *Plin1* would directly or indirectly influence the insulin signaling cascades, at least, in adipose tissue and skeletal muscle.

Macrophage depletion improves insulin resistance in Plin1$^{-/-}$ *mice*

Given that *Plin1* deficiency increased ATM numbers (Fig. 2) and induced insulin resistance (Fig. 6), we asked whether increased ATMs would be attributable for reduced insulin sensitivity in *Plin1*$^{-/-}$ mice. Clodronate liposomes successfully deplete phagocytic macrophages in peripheral tissues (34, 35). In eWAT from both *Plin1*$^{+/+}$ and *Plin1*$^{-/-}$ mice, clodronate treatment decreased the mRNA levels of *F4/80* and *Cd11c*, whereas the mRNA level of *Plin1* was not altered (Fig. 7*A*). Accordingly, microscopic analysis revealed that ATM accumulation was decreased by clodronate, and the difference in ATM contents between *Plin1*$^{+/+}$ and *Plin1*$^{-/-}$ mice was insignificant (Fig. 7*B*). As shown in Fig. 7, *C* and *D*, clodronate-mediated macrophage depletion improved insulin resistance of *Plin1*$^{-/-}$ mice to levels comparable with those observed in *Plin1*$^{+/+}$ mice. Together, these data suggested that enhanced macrophage recruitment and pro-inflammatory ATMs could mediate impaired insulin sensitivity in *Plin1*$^{-/-}$ mice.

Discussion

Immune cells are recruited to WAT under conditions that stimulate lipolysis. For instance, after overnight fasting, macrophage contents in WAT are increased (36, 37). Activation of adipocyte lipolysis with β_3-adrenergic agonists increases ATMs (36, 37). Inhibition of lipolysis by genetic ablation of *Atgl* prevents recruitment of macrophages to WAT (36, 37). However, it is not completely understood how lipolytic activation in adipocytes can increase ATMs. In this study, several lines of evidence supported that adipocyte *Plin1* represses pro-inflammatory responses in adipose tissue by restricting lipolysis. First, pro-inflammatory cytokine expression was higher in adipose tissues of *Plin1*$^{-/-}$ than in those of *Plin1*$^{+/+}$ mice. Second, macrophage contents were higher in adipose tissue of *Plin1*$^{-/-}$ mice. Third, *Plin1*-deficient adipocytes potentiated monocyte recruitment and macrophage activation. Last, suppression of the key lipases *Atgl* and *Hsl* in *Plin1*-deficient adipocytes alleviated monocyte migration, accompanied with reduced basal lipolysis. Furthermore, we observed that orlistat, a lipase inhibitor administration alleviated mRNA levels of macrophage marker genes and pro-inflammatory cytokines in eWAT of *Plin1*$^{-/-}$ mice (data not shown). Although orlistat primarily inhibits gastric and pancreatic lipases, it has been reported that orlistat represses lipolysis in adipocytes (38–41).

Upon metabolic states, adipose tissue secretes adipokines, which affect functional roles in several metabolic organs such as the liver, pancreas, skeletal muscle, brain, and immune system to modulate whole-body energy homeostasis. In obese animals, increased chemokines and inflammatory cytokines secreted from adipose tissue facilitate the recruitment of M1-type macrophages into adipose tissue (7). MCP-1 is a crucial chemokine for macrophage infiltration into adipose tissue. For example, adipocyte-specific *Mcp-1* transgenic mice exhibit increased ATMs and whole-body insulin resistance (42). It has been demonstrated that several lipid metabolites released from adipocytes or adipose tissue participate in inflammatory cell activation (15, 16, 32, 43, 44). Eicosanoids produced from adipocytes promote recruitment of immune cells (16, 32), whereas palmitoleate and palmitic acid-9-hydroxy stearic acid from adipose tissue reduce pro-inflammatory response in immune cells (15, 43, 44).

By-products of lipolysis, such as FFAs and eicosanoids, can induce adipose tissue inflammation. FFAs can activate pro-inflammatory responses in adipocytes and myeloid cells (17, 45). FFAs stimulate adipose tissue inflammation through the Toll-like receptor 4 signaling pathway, resulting in insulin resistance (17, 45). When adipocytes are treated with β_3-adrenergic ago-

Figure 5. Prostaglandins produced by *Plin1*$^{-/-}$ adipocytes promote monocyte migration. *A,* CM of SVC-derived adipocytes was collected and analyzed by LC-MS/MS lipidomic methods. Eicosanoid profiles were displayed as a heat map. *B,* the contents of PGD_2 and PGE_2 in the CM were assessed. *C,* pathway of prostaglandin synthesis from AA, and the involvement of COX. *D,* the level of intracellular AA in *Plin1*$^{+/+}$ or *Plin1*$^{-/-}$ adipocytes was measured by LC-MS/MS. **, $p < 0.01$ *versus Plin1*$^{+/+}$ group by Student's *t* test. *E–G,* SVC-derived adipocytes were transfected with control siRNA (*siCtl*) or *Cox2*-specific siRNA (*siCox2*). After 48 h, total RNA was extracted from siRNA-transfected SVC-derived adipocytes. The mRNA level of *Cox2* was analyzed by qRT-PCR. *, $p < 0.05$ *versus* siCtl group by two-way ANOVA followed by a post hoc Bonferroni test (*E*). The level of intracellular COX activity in *Plin1*$^{+/+}$ or *Plin1*$^{-/-}$ adipocytes was measured (*F*) and CM was collected from siRNA-transfected SVC-derived adipocytes. The number of migrated cells upon incubation with each CM was measured (*G*). *, $p < 0.05$; **, $p < 0.01$ *versus Plin1*$^{+/+}$, siCtl group by two-way ANOVA followed by a post hoc Bonferroni test. *H* and *I,* CM was collected from COX2 inhibitor, NS398 (1 μM), pretreated SVC-derived adipocytes. *H,* the level of secreted PGE_2 was measured by ELISA. ***, $p < 0.001$ *versus Plin1*$^{+/+}$, DMSO; ###, $p < 0.001$ *versus Plin1*$^{-/-}$, DMSO group by two-way ANOVA followed by Bonferroni's post hoc test. *I,* migrated cells upon incubation with PGE_2 (0.1 μM) supplemented CM were assessed. *, $p < 0.05$; ***, $p < 0.001$ *versus Plin1*$^{+/+}$, DMSO group; ###, $p < 0.001$ *versus Plin1*$^{-/-}$, DMSO group; $$, $p < 0.001$ *versus Plin1*$^{-/-}$, NS398 group by two-way ANOVA followed by Bonferroni's post hoc test. The levels of PGE_2 (*J*) and AA (*K*) in eWAT and serum PGE_2 levels (*L*) were measured. *, $p < 0.05$; ***, $p < 0.001$ *versus Plin1*$^{+/+}$ group by Student's *t* test. *M, Plin1*$^{+/+}$ or *Plin1*$^{-/-}$ mice were intraperitoneally administered daily with NS398 (10 mg/kg body weight) for 8 days. Relative mRNA levels of pro-inflammatory genes were determined in eWAT by qRT-PCR. *, $p < 0.05$; **, $p < 0.01$; ***, $p < 0.001$ *versus Plin1*$^{+/+}$, vehicle group; #, $p < 0.05$; ##, $p < 0.01$ *versus Plin1*$^{-/-}$, vehicle group by one-way ANOVA followed by Tukey's post hoc test. All data represent the mean ± S.E. All qRT-PCR data were normalized to the mRNA level of *cyclophilin*. *AD*, adipocytes; *Veh*, vehicle.

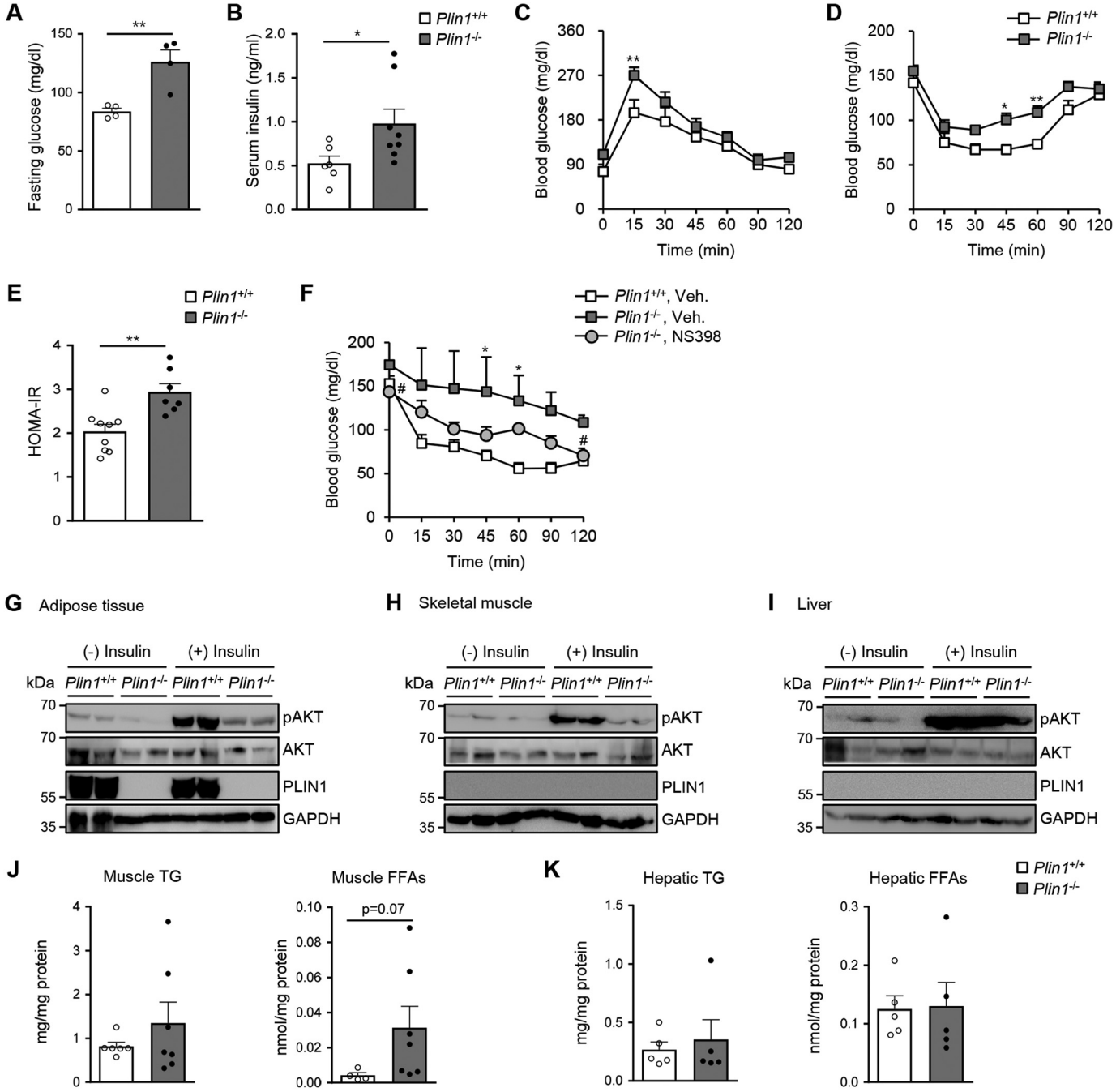

Figure 6. *Plin1*$^{-/-}$ mice show insulin resistance through lipid dysregulation. *A* and *B*, *Plin1*$^{+/+}$ and *Plin1*$^{-/-}$ mice were fasted for 15 h. Fasting serum glucose (*A*) and *ad libitum* insulin (*B*) were measured in *Plin1*$^{+/+}$ and *Plin1*$^{-/-}$ mice. *, $p < 0.05$; **, $p < 0.01$ *versus Plin1*$^{+/+}$ group by Student's *t* test. Intraperitoneal GTT (*C*) and ITT (*D*) were performed on *Plin1*$^{+/+}$ and *Plin1*$^{-/-}$ mice. *, $p < 0.05$; **, $p < 0.01$ *versus Plin1*$^{+/+}$ group by repeated-measures ANOVA (*RM-ANOVA*) followed by Bonferroni's post hoc test. *E,* homeostatic model assessment-insulin resistance (*HOMA-IR*) was measured in *Plin1*$^{+/+}$ and *Plin1*$^{-/-}$ mice. **, $p < 0.01$ *versus Plin1*$^{+/+}$ group by Student's *t* test. *F,* ITT was performed after treatment with NS398 (10 mg/kg body weight) for 7 days. *, $p < 0.05$ *versus Plin1*$^{+/+}$, vehicle group; #, $p < 0.05$ *versus Plin1*$^{-/-}$, vehicle group by RM-ANOVA followed by Bonferroni's post hoc test. *G–I, Plin1*$^{+/+}$ and *Plin1*$^{-/-}$ mice were injected with saline or insulin (0.75 units/kg body weight). Insulin signaling in eWAT (*G*), skeletal muscle (*H*), and liver (*I*) was assessed by immunoblot analysis using antibodies against pAKT (S473), AKT, PLIN1, and glyceraldehyde-3-phosphate dehydrogenase (*GAPDH*). Levels of TG and FFAs in skeletal muscle (*J*) or in liver (*K*) were measured. *p* value *versus Plin1*$^{+/+}$ mice by Student's *t* test. All data represent the mean ± S.E.

nists or forskolin to stimulate lipolysis, lipid metabolites generated from COX are elevated (16, 32). Administration of β_3-adrenergic agonist increases macrophage infiltration into WAT, which can be abrogated by COX2 inhibitor (16). Because *Plin1* in adipocytes plays an important role in the regulation of basal lipolysis (24), we assessed whether *Plin1* deficiency in adipocytes would change the repertoire of released lipid metabolites. The levels of secreted PGs such as PGE_2 were higher in *Plin1*-deficient adipocytes. Furthermore, we observed that suppression of PG production reduced monocyte migration. These data suggest that lipolytic by-products from *Plin1*$^{-/-}$ adipocytes could induce monocyte recruitment and macrophage activation to stimulate adipose tissue inflammation. Given that PGs are one of the potential mediators for pro-inflammatory

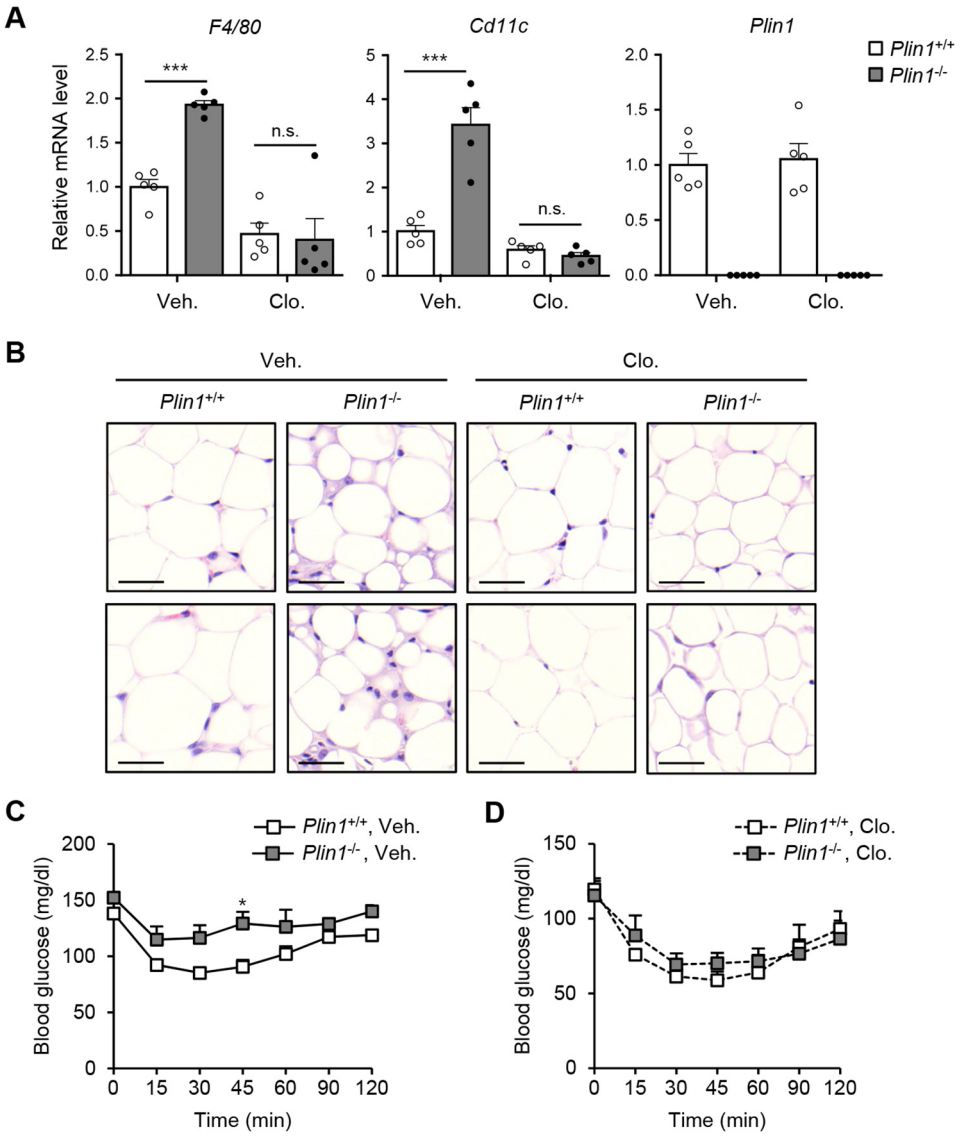

Figure 7. *Plin1*$^{-/-}$ mice exhibit improved insulin resistance upon macrophage depletion. *A* and *B*, clodronate (100 μl dose for 20–25 g of mouse) was intraperitoneally injected to *Plin1*$^{+/+}$ or *Plin1*$^{-/-}$ mice. Gene expression by qRT-PCR using macrophage markers (*A*) and histological analysis (*B*) are shown. *Scale bars*, 50 μm. ***, $p < 0.001$ *versus Plin1*$^{+/+}$, vehicle group by two way-ANOVA followed by Bonferroni's post hoc test. *C* and *D*, ITT was performed 4 days after the injection of clodronate. *, $p < 0.05$ *versus Plin1*$^{+/+}$, vehicle group by repeated measures-ANOVA followed by Bonferroni's post hoc test. All data represent the mean ± S.E. All qRT-PCR data were normalized to the mRNA level of *cyclophilin*. *Veh*, vehicle; *Clo*, clodronate; *N.S.*, not significant.

responses in *Plin1*$^{-/-}$ mice, it is plausible to speculate that *Plin1* in adipose tissue could play a pivotal role in maintaining immune balance, which might eventually contribute to metabolic homeostasis.

It has been suggested that the Plin family could be associated with inflammatory responses (46–53). For example, *Plin1* ablation in *Ldlr*$^{-/-}$ mice led to an increase in atherosclerotic lesion area when compared with *Ldlr*$^{-/-}$ mice (46). In addition, Zou *et al.* (47) reported that 20-week-old *Plin1*$^{-/-}$ mice in the 129/SvEv background developed spontaneous hypertension with perivascular adipose tissue (PVAT) dysfunction. The anti-contractile effect was impaired in PVAT of *Plin1*$^{-/-}$ mice compared with that of *Plin1*$^{+/+}$ mice. Moreover, pro-inflammatory gene expression and macrophage markers of PVAT were up-regulated by *Plin1* deletion (47). However, it remains unclear which factors could regulate the inflammatory response in PVAT of *Plin1*$^{-/-}$ mice. We found that NCD-fed lean *Plin1*$^{-/-}$ mice showed enhanced adipose tissue inflammation, which would reduce whole-body insulin sensitivity. In adipose tissue of *Plin1*$^{-/-}$ mice, total macrophages and the CD11c^{+} M1-type macrophage population were elevated. Moreover, it is very likely that certain lipid metabolites secreted from *Plin1*$^{-/-}$ adipocytes would enhance monocyte recruitment and pro-inflammatory responses in macrophages. Furthermore, macrophage depletion using clodronate restored insulin sensitivity in *Plin1*$^{-/-}$ mice. Collectively, these data suggest that ATM stimulation by *Plin1* deficiency seems to be critical for systemic insulin resistance in *Plin1*$^{-/-}$ mice (Fig. 8). Nevertheless, we cannot exclude the possibility that *Plin1* ablation might induce systemic insulin resistance through alternative pathways. For instance, COX2 inhibition ameliorated adipose tissue inflammation (Fig. 5) even though COX2 inhibition did not thoroughly improve insulin resistance in *Plin1*$^{-/-}$ mice (Fig. 6). Furthermore, elevation of circulating TG and FFAs has delete-

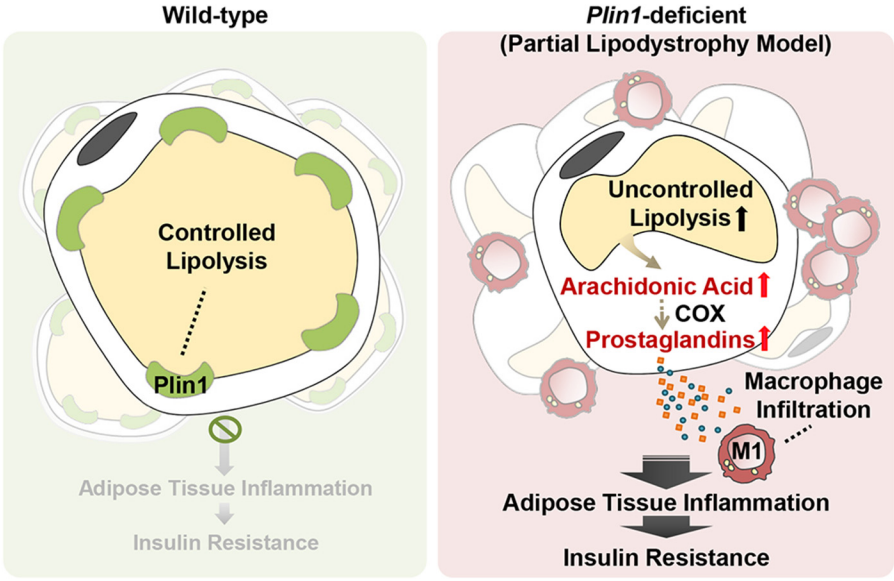

Figure 8. Proposed model. In *Plin1*-deficient adipose tissue, lipolytic by-products such as prostaglandins promote adipose tissue inflammation, contributing to whole-body insulin resistance.

rious effects in non-adipose tissue by inducing lipotoxicity. Impaired insulin signaling reportedly is associated with increased uptake of FFAs into muscle (54). In this regard, we observed that serum levels of TG and FFAs were elevated in *Plin1*$^{-/-}$ mice. Moreover, in skeletal muscle of *Plin1*$^{-/-}$ mice, intracellular TG and FFA levels were slightly higher and insulin signaling pathways were impaired (Fig. 6). Thus, it remains to be elucidated whether deteriorated insulin sensitivity in *Plin1*$^{-/-}$ mice might, at least in part result from lipotoxicity in peripheral tissues.

Several pathological conditions, such as lipodystrophy and cachexia, are closely linked to insulin resistance, lipid dysregulation, and inflammation, accompanied with decreased adiposity (55, 56). Interestingly, studies on human *PLIN1* deficiency have suggested that mutations in *PLIN1* could be responsible for autosomal dominant partial lipodystrophy. Gandotra *et al.* (9) identified two heterozygous frameshift mutations in *PLIN1*. Both mutations result in insulin resistance, severe dyslipidemia, and partial lipodystrophy (9). Compared with healthy subjects, adipocyte size is significantly decreased, and macrophage infiltration is elevated in adipose tissues of lipodystrophic patients (9). We found that lean *Plin1*$^{-/-}$ mice showed phenotypes similar to those of *PLIN1* mutant patients. In particular, *Plin1*$^{-/-}$ mice exhibited decreased fat mass, dyslipidemia, and insulin resistance, which are common symptoms of lipodystrophic patients. Cachexia is considered a metabolic disorder and is characterized by loss of adipose tissue and skeletal muscle. Adipose tissue loss in cancer cachexia might be partly a consequence of increased lipolysis, and this alteration in lipid metabolism is closely associated with adipose tissue inflammation (57–59). These findings raise the possibility that dysregulated lipid metabolism of adipose tissue would affect systemic insulin resistance in lipodystrophic and cachectic subjects. Moreover, metabolically unhealthy lean individuals present impaired insulin sensitivity and exhibit higher serum TG and FFA levels than metabolically healthy lean individuals (60, 61). Serum levels of inflammatory markers including TNFα, interleukin-6, and MCP-1 are higher in metabolically unhealthy lean subjects than in metabolically healthy lean subjects (62, 63). However, it is unclear how metabolically unhealthy lean individuals fail to maintain whole-body metabolic homeostasis due to the lack of proper animal models. Therefore, the present data indicate that *Plin1*$^{-/-}$ mice could be a suitable model to investigate the causality between insulin resistance and adipose tissue inflammation as well as lipid dysregulation in metabolically unhealthy lean subjects.

In conclusion, we identified novel roles of *Plin1* in adipose tissue inflammation and insulin sensitivity in lean animals. Our data suggest that *Plin1* is a key regulator against adipose tissue inflammation and insulin resistance by restricting lipolysis. Taken together, *Plin1*-mediated lipid metabolism might be a potential target to treat inflammation-linked metabolic diseases as well as lipid dysregulation.

Experimental procedures

Animals and treatments

The animal study and experimental procedures were approved by the Seoul National University Institutional Animal Care and Use Committee. *Plin1*$^{-/-}$ mice in a pure C57BL/6 background were obtained from Alan R. Kimmel (National Institutes of Health, Bethesda, MD). Mice were housed under a 12-h light/12-h dark cycle. Heterozygous mice were bred to generate *Plin1*$^{+/+}$ and *Plin1*$^{-/-}$ littermates. *Plin1*$^{+/+}$ and *Plin1*$^{-/-}$ mice were maintained on NCD. Nine- to 12-week-old male mice were used for experiments, except where indicated. At 9–11 weeks of age, *Plin1*$^{+/+}$ and *Plin1*$^{-/-}$ mice were intraperitoneally injected with vehicle (1% DMSO in PBS), NS398 (10 mg/kg of body weight, Cayman Chemical) daily for 8 days. For intraperitoneal GTT, 17-week-old mice were fasted overnight and then administered glucose (1 g/kg of body weight). For ITT, mice were intraperitoneally injected with insulin (0.75

unit/kg of body weight). To test insulin signaling *in vivo*, mice were fasted overnight and killed 15 min after injection of PBS or insulin (0.75 unit/kg body weight). Adipose tissue, skeletal muscle, and liver were isolated and quickly frozen for Western blot analysis. For macrophage depletion, clodronate liposomes (FormuMax Scientific) were intraperitoneally injected once.

Serum profiling

Serum FFA, TG, and cholesterol levels were assessed using FFA (Roche Applied Science), TG (Thermo Fisher Scientific), and cholesterol (Thermo Fisher Scientific) quantification kits. Serum insulin, MCP-1, and TNFα levels were measured using insulin (Morinaga Institute of Biological Science Inc.), MCP-1 (Invitrogen), and TNFα (Invitrogen) ELISA kits.

Adipose tissue fractionation

Adipose tissue was fractionated as described previously (64). Briefly, eWAT was dissected out, chopped, incubated in collagenase buffer (0.1 M HEPES, 0.125 M NaCl, 5 mM KCl, 1.3 mM $CaCl_2$, 5 mM glucose, 1.5% (w/v) glucose, and 0.1% (w/v) collagenase I) for 20 min at 37 °C with shaking, and centrifuged. Supernatants containing adipocytes were used for primary cell culture. Pelleted SVC fractions were used for flow cytometry and SVC-derived adipocyte differentiation.

Flow cytometry

Flow cytometric analysis was performed as described previously (65). SVC fractions were separated from red blood cells by adding lysis buffer (155 mM NH_4Cl, 0.1 M Tris-HCl (pH 7.65) (9:1)). SVCs were stained with monoclonal antibodies against CD11b (BD Biosciences), F4/80, CD11c, and CD206 (eBioscience) for macrophage analysis using a FACS Canto II (BD Biosciences).

SVC-derived adipocyte differentiation

Pre-adipocytes were grown to confluence (day 0) in induction medium consisting of Dulbecco's modified Eagle's medium (DMEM), 10% fetal bovine serum (FBS), 167 nM insulin, 1 μM 3,3′,5-triiodo-L-thyronine, 2 μM rosiglitazone, 52 μM isobutylmethylxanthine, and 1 μM dexamethasone. After a 2-day incubation in induction medium, the cells were transferred to differentiation medium (DMEM, 10% FBS, 167 nM insulin, 1 μM 3,3′,5-triiodo-L-thyronine, and 2 μM rosiglitazone), which was changed every other day. For siRNA transfection, differentiated adipocytes were transfected by Lipofectamine 2000 (Invitrogen) according to the manufacturer's protocol.

Isolation of peritoneal macrophages

Mice were intraperitoneally injected with sterile thioglycollate solution (3 ml/mouse). After 3 days, peritoneal cells were harvested by washing the peritoneal cavity with PBS. Primary peritoneal macrophages were cultured in DMEM containing 10% FBS to allow the cells to adhere. Nonadherent cells were removed by washing.

Co-culture and CM preparation

Co-culture experiments were conducted as described previously (35). For indirect co-culture experiments, chopped eWAT or primary adipocytes were placed in the lower chambers of Transwell plates (0.4 μm pore size) and co-cultured with peritoneal macrophages in the upper chambers. After 48 h incubation, the macrophages were used for RNA extraction. For CM preparation, chopped eWAT or primary adipocytes were incubated in serum-free DMEM for 48 h and CM was collected. To test THP-1 or peritoneal macrophage migration, Transwell inserts (8 μm pore size) were used. THP-1 monocytes or macrophages were loaded in the upper chambers and CM was placed in the lower chambers. After 6 h, the degree of cell migration was determined as the number of cells in the lower chambers.

Global metabolome profiling

Lipids were extracted from CM using conventional procedures (66). A LC–MS system equipped with Ultimate3000 (Dionex), Orbitrap XL (Thermo Fisher Scientific), and reverse phase column (Pursuit 5 200 × 2.0 mm) was used. Mobile phase A was 0.1% formic acid in H_2O, and mobile phase B was 0.1% formic acid in methanol. The flow rate was 400 μl/min and the column temperature was 25 °C. Data were analyzed using Seive 2 and MetaboAnalyst. Metabolite features containing m/z and retention time were extracted using Seive 2.2. Data were statistically analyzed using MetaboAnalyst. Metabolite features were identified using METLIN DB with mass accuracy of 10 ppm.

Eicosanoid analysis

Eicosanoids were extracted from CM, cells, and eWAT using solid-phase extraction, as described (67). A LC-tandem MS system equipped with 1290 HPLC (Agilent), Qtrap 5500 (ABSciex), and reverse phase column (Pursuit 5 200 × 2.0 mm) was used. Mobile phase A was 0.1% acetic acid in H_2O and mobile phase B was 0.1% acetic acid in acetonitrile/MeOH (84/16, v/v). The flow rate was 250 μl/min and the column temperature was 25 °C. The multiple reaction monitoring mode was used in negative ion mode, and the extracted ion chromatogram corresponding to the specific transition of each analyte was used for quantification. The calibration range for each analyte was 0.1–1000 nM ($r^2 \geq 0.99$).

COX activity assay and PGE_2 measurement

The COX activity was assayed using a colorimetric assay kit (Cayman Chemical) according to the manufacturer's guidelines. PGE_2, selective COX2 inhibitor NS398, and PGE_2 ELISA kits were purchased from Cayman Chemical.

Quantitative reverse transcription (qRT)-PCR

Total RNA was isolated from eWAT, macrophages, and SVC-derived adipocytes. cDNA was synthesized using a reverse transcriptase kit (Thermo Fisher Scientific) according to the manufacturer's instructions. Primers used for qRT-PCR were obtained from Bioneer (South Korea).

Western blot analysis

eWAT, skeletal muscle, liver, and SVC-derived adipocytes were lysed with TGN lysis buffer (50 mM Tris (pH 7.5), 150 mM NaCl, 1% Tween 20, 0.2% Nonidet P-40, 1 mM phenylmethylsulfonyl fluoride, 1 mM NaF, 1 mM Na_3VO_4 and protease inhib-

itor mixture from GenDEPOT). Proteins in the lysates were separated by SDS-PAGE and transferred to polyvinylidene fluoride membranes (Millipore). The blots were blocked with 5% nonfat milk and probed with anti-pAKT (S473; Cell Signaling Technology), anti-AKT (BD Bioscience), or anti-PLIN1 (23).

Statistical analysis

All data were analyzed using Student's *t* test or analysis of variance (ANOVA) in Excel (Microsoft) or GraphPad Prism; *p* values of <0.05 were considered significant.

Author contributions—J. H. S. conceptualization; J. H. S. and S. J. K. investigation; J. H. S. writing-original draft; J. H. S., S. S. C., and J. B. K. writing-review and editing; Y. K. L. and J. S. H. validation; Y. G. J. and H. J. Y. data curation; Y. G. J., J. I. K., and H. J. Y. software; J. I. K. visualization; S. J. K. methodology; J. B. K. supervision; J. B. K. project administration.

Acknowledgments—We thank Constantine Londos who produced the Plin1-deficient mouse model and anti-PLIN1 antibody, and Alan R. Kimmel at the United States National Institutes of Health, who provided these materials.

References

1. Kwon, H., and Pessin, J. E. (2013) Adipokines mediate inflammation and insulin resistance. *Front. Endocrinol. (Lausanne)* **4,** 71 Medline
2. Olefsky, J. M., and Glass, C. K. (2010) Macrophages, inflammation, and insulin resistance. *Annu. Rev. Physiol.* **72,** 219–246 CrossRef Medline
3. Lumeng, C. N., DelProposto, J. B., Westcott, D. J., and Saltiel, A. R. (2008) Phenotypic switching of adipose tissue macrophages with obesity is generated by spatiotemporal differences in macrophage subtypes. *Diabetes* **57,** 3239–3246 CrossRef Medline
4. Weisberg, S. P., McCann, D., Desai, M., Rosenbaum, M., Leibel, R. L., and Ferrante, A. W., Jr. (2003) Obesity is associated with macrophage accumulation in adipose tissue. *J. Clin. Invest.* **112,** 1796–1808 CrossRef Medline
5. Xu, H., Barnes, G. T., Yang, Q., Tan, G., Yang, D., Chou, C. J., Sole, J., Nichols, A., Ross, J. S., Tartaglia, L. A., and Chen, H. (2003) Chronic inflammation in fat plays a crucial role in the development of obesity-related insulin resistance. *J. Clin. Invest.* **112,** 1821–1830 CrossRef Medline
6. Lumeng, C. N., Deyoung, S. M., Bodzin, J. L., and Saltiel, A. R. (2007) Increased inflammatory properties of adipose tissue macrophages recruited during diet-induced obesity. *Diabetes* **56,** 16–23 CrossRef Medline
7. Hotamisligil, G. S., Shargill, N. S., and Spiegelman, B. M. (1993) Adipose expression of tumor necrosis factor-α: direct role in obesity-linked insulin resistance. *Science* **259,** 87–91 CrossRef Medline
8. Herrero, L., Shapiro, H., Nayer, A., Lee, J., and Shoelson, S. E. (2010) Inflammation and adipose tissue macrophages in lipodystrophic mice. *Proc. Natl. Acad. Sci. U.S.A.* **107,** 240–245 CrossRef Medline
9. Gandotra, S., Le Dour, C., Bottomley, W., Cervera, P., Giral, P., Reznik, Y., Charpentier, G., Auclair, M., Delépine, M., Barroso, I., Semple, R. K., Lathrop, M., Lascols, O., Capeau, J., O'Rahilly, S., *et al.* (2011) Perilipin deficiency and autosomal dominant partial lipodystrophy. *N. Engl. J. Med.* **364,** 740–748 CrossRef Medline
10. Martin, S., Fernandez-Rojo, M. A., Stanley, A. C., Bastiani, M., Okano, S., Nixon, S. J., Thomas, G., Stow, J. L., and Parton, R. G. (2012) Caveolin-1 deficiency leads to increased susceptibility to cell death and fibrosis in white adipose tissue: characterization of a lipodystrophic model. *PLoS ONE* **7,** e46242 CrossRef Medline
11. de Matos-Neto, E. M., Lima, J. D., de Pereira, W. O., Figuerêdo, R. G., Riccardi, D. M., Radloff, K., das Neves, R. X., Camargo, R. G., Maximiano, L. F., Tokeshi, F., Otoch, J. P., Goldszmid, R., Câmara, N. O., Trinchieri, G., de Alcântara, P. S., and Seelaender, M. (2015) Systemic inflammation in cachexia: is tumor cytokine expression profile the culprit? *Front. Immunol.* **6,** 629 Medline
12. Batista, M. L., Jr., Henriques, F. S., Neves, R. X., Olivan, M. R., Matos-Neto, E. M., Alcântara, P. S., Maximiano, L. F., Otoch, J. P., Alves, M. J., and Seelaender, M. (2016) Cachexia-associated adipose tissue morphological rearrangement in gastrointestinal cancer patients. *J. Cachexia Sarcopenia Muscle* **7,** 37–47 CrossRef Medline
13. Bensinger, S. J., and Tontonoz, P. (2008) Integration of metabolism and inflammation by lipid-activated nuclear receptors. *Nature* **454,** 470–477 CrossRef Medline
14. Shimizu, T. (2009) Lipid mediators in health and disease: enzymes and receptors as therapeutic targets for the regulation of immunity and inflammation. *Annu. Rev. Pharmacol. Toxicol.* **49,** 123–150 CrossRef Medline
15. Yore, M. M., Syed, I., Moraes-Vieira, P. M., Zhang, T., Herman, M. A., Homan, E. A., Patel, R. T., Lee, J., Chen, S., Peroni, O. D., Dhaneshwar, A. S., Hammarstedt, A., Smith, U., McGraw, T. E., Saghatelian, A., and Kahn, B. B. (2014) Discovery of a class of endogenous mammalian lipids with anti-diabetic and anti-inflammatory effects. *Cell* **159,** 318–332 CrossRef Medline
16. Gartung, A., Zhao, J., Chen, S., Mottillo, E., VanHecke, G. C., Ahn, Y. H., Maddipati, K. R., Sorokin, A., Granneman, J., and Lee, M. J. (2016) Characterization of eicosanoids produced by adipocyte lipolysis: implication of cyclooxygenase-2 in adipose inflammation. *J. Biol. Chem.* **291,** 16001–16010 CrossRef Medline
17. Suganami, T., Tanimoto-Koyama, K., Nishida, J., Itoh, M., Yuan, X., Mizuarai, S., Kotani, H., Yamaoka, S., Miyake, K., Aoe, S., Kamei, Y., and Ogawa, Y. (2007) Role of the Toll-like receptor 4/NF-κB pathway in saturated fatty acid-induced inflammatory changes in the interaction between adipocytes and macrophages. *Arterioscler. Thromb. Vasc. Biol.* **27,** 84–91 CrossRef Medline
18. Li, P., Oh, D. Y., Bandyopadhyay, G., Lagakos, W. S., Talukdar, S., Osborn, O., Johnson, A., Chung, H., Maris, M., Ofrecio, J. M., Taguchi, S., Lu, M., and Olefsky, J. M. (2015) LTB4 promotes insulin resistance in obese mice by acting on macrophages, hepatocytes and myocytes. *Nat. Med.* **21,** 239–247 CrossRef Medline
19. Carman, G. M. (2012) Thematic minireview series on the lipid droplet, a dynamic organelle of biomedical and commercial importance. *J. Biol. Chem.* **287,** 2272 CrossRef Medline
20. Kimmel, A. R., and Sztalryd, C. (2016) The perilipins: major cytosolic lipid droplet-associated proteins and their roles in cellular lipid storage, mobilization, and systemic homeostasis. *Annu. Rev. Nutr.* **36,** 471–509 CrossRef Medline
21. Hoo, R. L., Shu, L., Cheng, K. K., Wu, X., Liao, B., Wu, D., Zhou, Z., and Xu, A. (2017) Adipocyte fatty acid binding protein potentiates toxic lipids-induced endoplasmic reticulum stress in macrophages via inhibition of Janus kinase 2-dependent autophagy. *Sci. Rep.* **7,** 40657 CrossRef Medline
22. Iyer, A., Fairlie, D. P., Prins, J. B., Hammock, B. D., and Brown, L. (2010) Inflammatory lipid mediators in adipocyte function and obesity. *Nat. Rev. Endocrinol.* **6,** 71–82 CrossRef Medline
23. Greenberg, A. S., Egan, J. J., Wek, S. A., Garty, N. B., Blanchette-Mackie, E. J., and Londos, C. (1991) Perilipin, a major hormonally regulated adipocyte-specific phosphoprotein associated with the periphery of lipid storage droplets. *J. Biol. Chem.* **266,** 11341–11346 Medline
24. Tansey, J. T., Sztalryd, C., Gruia-Gray, J., Roush, D. L., Zee, J. V., Gavrilova, O., Reitman, M. L., Deng, C. X., Li, C., Kimmel, A. R., and Londos, C. (2001) Perilipin ablation results in a lean mouse with aberrant adipocyte lipolysis, enhanced leptin production, and resistance to diet-induced obesity. *Proc. Natl. Acad. Sci. U.S.A.* **98,** 6494–6499 CrossRef Medline
25. Miyoshi, H., Souza, S. C., Zhang, H. H., Strissel, K. J., Christoffolete, M. A., Kovsan, J., Rudich, A., Kraemer, F. B., Bianco, A. C., Obin, M. S., and Greenberg, A. S. (2006) Perilipin promotes hormone-sensitive lipase-mediated adipocyte lipolysis via phosphorylation-dependent and -independent mechanisms. *J. Biol. Chem.* **281,** 15837–15844 CrossRef Medline
26. Brasaemle, D. L., Levin, D. M., Adler-Wailes, D. C., and Londos, C. (2000) The lipolytic stimulation of 3T3-L1 adipocytes promotes the transloca-

tion of hormone-sensitive lipase to the surfaces of lipid storage droplets. *Biochim. Biophys. Acta* **1483,** 251–262 CrossRef Medline

27. Granneman, J. G., Moore, H. P., Krishnamoorthy, R., and Rathod, M. (2009) Perilipin controls lipolysis by regulating the interactions of AB-hydrolase containing 5 (Abhd5) and adipose triglyceride lipase (Atgl). *J. Biol. Chem.* **284,** 34538–34544 CrossRef Medline
28. Gaidhu, M. P., Anthony, N. M., Patel, P., Hawke, T. J., and Ceddia, R. B. (2010) Dysregulation of lipolysis and lipid metabolism in visceral and subcutaneous adipocytes by high-fat diet: role of ATGL, HSL, and AMPK. *Am. J. Physiol. Cell Physiol* **298,** C961–971 CrossRef Medline
29. Fujisaka, S., Usui, I., Bukhari, A., Ikutani, M., Oya, T., Kanatani, Y., Tsuneyama, K., Nagai, Y., Takatsu, K., Urakaze, M., Kobayashi, M., and Tobe, K. (2009) Regulatory mechanisms for adipose tissue M1 and M2 macrophages in diet-induced obese mice. *Diabetes* **58,** 2574–2582 CrossRef Medline
30. Oh, D. Y., Morinaga, H., Talukdar, S., Bae, E. J., and Olefsky, J. M. (2012) Increased macrophage migration into adipose tissue in obese mice. *Diabetes* **61,** 346–354 CrossRef Medline
31. Ayache, S., Panelli, M. C., Byrne, K. M., Slezak, S., Leitman, S. F., Marincola, F. M., and Stroncek, D. F. (2006) Comparison of proteomic profiles of serum, plasma, and modified media supplements used for cell culture and expansion. *J. Transl. Med.* **4,** 40 CrossRef Medline
32. Hu, X., Cifarelli, V., Sun, S., Kuda, O., Abumrad, N. A., and Su, X. (2016) Major role of adipocyte prostaglandin E2 in lipolysis-induced macrophage recruitment. *J. Lipid Res.* **57,** 663–673 CrossRef Medline
33. Vane, J. R., Bakhle, Y. S., and Botting, R. M. (1998) Cyclooxygenases 1 and 2. *Annu. Rev. Pharmacol. Toxicol.* **38,** 97–120 CrossRef Medline
34. Feng, B., Jiao, P., Nie, Y., Kim, T., Jun, D., van Rooijen, N., Yang, Z., and Xu, H. (2011) Clodronate liposomes improve metabolic profile and reduce visceral adipose macrophage content in diet-induced obese mice. *PLoS ONE* **6,** e24358 CrossRef Medline
35. Choe, S. S., Shin, K. C., Ka, S., Lee, Y. K., Chun, J. S., and Kim, J. B. (2014) Macrophage HIF-2α ameliorates adipose tissue inflammation and insulin resistance in obesity. *Diabetes* **63,** 3359–3371 CrossRef Medline
36. Kosteli, A., Sugaru, E., Haemmerle, G., Martin, J. F., Lei, J., Zechner, R., and Ferrante, A. W., Jr. (2010) Weight loss and lipolysis promote a dynamic immune response in murine adipose tissue. *J. Clin. Invest.* **120,** 3466–3479 CrossRef Medline
37. Schoiswohl, G., Stefanovic-Racic, M., Menke, M. N., Wills, R. C., Surlow, B. A., Basantani, M. K., Sitnick, M. T., Cai, L., Yazbeck, C. F., Stolz, D. B., Pulinilkunnil, T., O'Doherty, R. M., and Kershaw, E. E. (2015) Impact of reduced ATGL-mediated adipocyte lipolysis on obesity-associated insulin resistance and inflammation in male mice. *Endocrinology* **156,** 3610–3624 CrossRef Medline
38. Hadváry, P., Lengsfeld, H., and Wolfer, H. (1988) Inhibition of pancreatic lipase *in vitro* by the covalent inhibitor tetrahydrolipstatin. *Biochem. J.* **256,** 357–361 CrossRef Medline
39. Iglesias, J., Lamontagne, J., Erb, H., Gezzar, S., Zhao, S., Joly, E., Truong, V. L., Skorey, K., Crane, S., Madiraju, S. R., and Prentki, M. (2016) Simplified assays of lipolysis enzymes for drug discovery and specificity assessment of known inhibitors. *J. Lipid Res.* **57,** 131–141 CrossRef Medline
40. Gauthier, M. S., Miyoshi, H., Souza, S. C., Cacicedo, J. M., Saha, A. K., Greenberg, A. S., and Ruderman, N. B. (2008) AMP-activated protein kinase is activated as a consequence of lipolysis in the adipocyte: potential mechanism and physiological relevance. *J. Biol. Chem.* **283,** 16514–16524 CrossRef Medline
41. Lee, J. H., Han, J. S., Kong, J., Ji, Y., Lv, X., Lee, J., Li, P., and Kim, J. B. (2016) Protein kinase A subunit balance regulates lipid metabolism in *Caenorhabditis elegans* and mammalian adipocytes. *J. Biol. Chem.* **291,** 20315–20328 CrossRef Medline
42. Kanda, H., Tateya, S., Tamori, Y., Kotani, K., Hiasa, K., Kitazawa, R., Kitazawa, S., Miyachi, H., Maeda, S., Egashira, K., and Kasuga, M. (2006) MCP-1 contributes to macrophage infiltration into adipose tissue, insulin resistance, and hepatic steatosis in obesity. *J. Clin. Invest.* **116,** 1494–1505 CrossRef Medline
43. Cao, H., Gerhold, K., Mayers, J. R., Wiest, M. M., Watkins, S. M., and Hotamisligil, G. S. (2008) Identification of a lipokine, a lipid hormone linking adipose tissue to systemic metabolism. *Cell* **134,** 933–944 CrossRef Medline
44. Chan, K. L., Pillon, N. J., Sivaloganathan, D. M., Costford, S. R., Liu, Z., Théret, M., Chazaud, B., and Klip, A. (2015) Palmitoleate reverses high fat-induced proinflammatory macrophage polarization via AMP-activated protein kinase (AMPK). *J. Biol. Chem.* **290,** 16979–16988 CrossRef Medline
45. Yeop Han, C., Kargi, A. Y., Omer, M., Chan, C. K., Wabitsch, M., O'Brien, K. D., Wight, T. N., and Chait, A. (2010) Differential effect of saturated and unsaturated free fatty acids on the generation of monocyte adhesion and chemotactic factors by adipocytes: dissociation of adipocyte hypertrophy from inflammation. *Diabetes* **59,** 386–396 CrossRef Medline
46. Langlois, D., Forcheron, F., Li, J. Y., del Carmine, P., Neggazi, S., and Beylot, M. (2011) Increased atherosclerosis in mice deficient in perilipin1. *Lipids Health Dis* **10,** 169 CrossRef Medline
47. Zou, L., Wang, W., Liu, S., Zhao, X., Lyv, Y., Du, C., Su, X., Geng, B., and Xu, G. (2016) Spontaneous hypertension occurs with adipose tissue dysfunction in perilipin-1 null mice. *Biochim. Biophys. Acta* **1862,** 182–191 CrossRef Medline
48. Zhang, S., Liu, G., Xu, C., Liu, L., Zhang, Q., Xu, Q., Jia, H., Li, X., and Li, X. (2018) Perilipin 1 mediates lipid metabolism homeostasis and inhibits inflammatory cytokine synthesis in bovine adipocytes. *Front. Immunol.* **9,** 467 CrossRef Medline
49. Yamamoto, K., Miyoshi, H., Cho, K. Y., Nakamura, A., Greenberg, A. S., and Atsumi, T. (2018) Overexpression of perilipin1 protects against atheroma progression in apolipoprotein E knockout mice. *Atherosclerosis* **269,** 192–196 CrossRef Medline
50. McManaman, J. L., Bales, E. S., Orlicky, D. J., Jackman, M., MacLean, P. S., Cain, S., Crunk, A. E., Mansur, A., Graham, C. E., Bowman, T. A., and Greenberg, A. S. (2013) Perilipin-2-null mice are protected against diet-induced obesity, adipose inflammation, and fatty liver disease. *J. Lipid Res.* **54,** 1346–1359 CrossRef Medline
51. Najt, C. P., Senthivinayagam, S., Aljazi, M. B., Fader, K. A., Olenic, S. D., Brock, J. R., Lydic, T. A., Jones, A. D., and Atshaves, B. P. (2016) Liver-specific loss of Perilipin 2 alleviates diet-induced hepatic steatosis, inflammation, and fibrosis. *Am. J. Physiol. Gastrointest. Liver Physiol.* **310,** G726–738 CrossRef Medline
52. Zhou, P. L., Li, M., Han, X. W., Bi, Y. H., Zhang, W. G., Wu, Z. Y., and Wu, G. (2017) Plin5 deficiency promotes atherosclerosis progression through accelerating inflammation, apoptosis and oxidative stress. *J. Cell. Biochem.* CrossRef
53. Montgomery, M. K., Mokhtar, R., Bayliss, J., Parkington, H. C., Suturin, V. M., Bruce, C. R., and Watt, M. J. (2018) Perilipin 5 deletion unmasks an endoplasmic reticulum stress-fibroblast growth factor 21 axis in skeletal muscle. *Diabetes* **67,** 594–606 CrossRef Medline
54. Petersen, K. F., and Shulman, G. I. (2002) Pathogenesis of skeletal muscle insulin resistance in type 2 diabetes mellitus. *Am. J. Cardiol.* **90,** 11–18 Medline
55. Savage, D. B. (2009) Mouse models of inherited lipodystrophy. *Dis. Model Mech.* **2,** 554–562 CrossRef Medline
56. Porporato, P. E. (2016) Understanding cachexia as a cancer metabolism syndrome. *Oncogenesis* **5,** e200 CrossRef Medline
57. Klein, S., and Wolfe, R. R. (1990) Whole-body lipolysis and triglyceride-fatty acid cycling in cachectic patients with esophageal cancer. *J. Clin. Invest.* **86,** 1403–1408 CrossRef Medline
58. Das, S. K., Eder, S., Schauer, S., Diwoky, C., Temmel, H., Guertl, B., Gorkiewicz, G., Tamilarasan, K. P., Kumari, P., Trauner, M., Zimmermann, R., Vesely, P., Haemmerle, G., Zechner, R., and Hoefler, G. (2011) Adipose triglyceride lipase contributes to cancer-associated cachexia. *Science* **333,** 233–238 CrossRef Medline
59. Batista, M. L., Jr, Peres, S. B., McDonald, M. E., Alcantara, P. S., Olivan, M., Otoch, J. P., Farmer, S. R., and Seelaender, M. (2012) Adipose tissue inflammation and cancer cachexia: possible role of nuclear transcription factors. *Cytokine* **57,** 9–16 CrossRef Medline
60. Succurro, E., Marini, M. A., Frontoni, S., Hribal, M. L., Andreozzi, F., Lauro, R., Perticone, F., and Sesti, G. (2008) Insulin secretion in metabolically obese, but normal weight, and in metabolically healthy but obese individuals. *Obesity (Silver Spring)* **16,** 1881–1886 Medline

61. Kim, M., Paik, J. K., Kang, R., Kim, S. Y., Lee, S. H., and Lee, J. H. (2013) Increased oxidative stress in normal-weight postmenopausal women with metabolic syndrome compared with metabolically healthy overweight/obese individuals. *Metabolism* **62,** 554–560 CrossRef Medline
62. Indulekha, K., Surendar, J., Anjana, R. M., Geetha, L., Gokulakrishnan, K., Pradeepa, R., and Mohan, V. (2015) Metabolic obesity, adipocytokines, and inflammatory markers in Asian Indians: CURES-124. *Diabetes Technol. Ther.* **17,** 134–141 CrossRef Medline
63. De Lorenzo, A., Del Gobbo, V., Premrov, M. G., Bigioni, M., Galvano, F., and Di Renzo, L. (2007) Normal-weight obese syndrome: early inflammation? *Am. J. Clin. Nutr.* **85,** 40–45 CrossRef Medline
64. Ham, M., Choe, S. S., Shin, K. C., Choi, G., Kim, J. W., Noh, J. R., Kim, Y. H., Ryu, J. W., Yoon, K. H., Lee, C. H., and Kim, J. B. (2016) Glucose-6-phosphate dehydrogenase deficiency improves insulin resistance with reduced adipose tissue inflammation in obesity. *Diabetes* **65,** 2624–2638 CrossRef Medline
65. Huh, J. Y., Park, J., Kim, J. I., Park, Y. J., Lee, Y. K., and Kim, J. B. (2017) deletion of CD1d in adipocytes aggravates adipose tissue inflammation and insulin resistance in obesity. *Diabetes* **66,** 835–847 CrossRef Medline
66. Folch, J., Lees, M., and Sloane Stanley, G. H. (1957) A simple method for the isolation and purification of total lipides from animal tissues. *J. Biol. Chem.* **226,** 497–509 Medline
67. Yang, J., Schmelzer, K., Georgi, K., and Hammock, B. D. (2009) Quantitative profiling method for oxylipin metabolome by liquid chromatography electrospray ionization tandem mass spectrometry. *Anal. Chem.* **81,** 8085–8093 CrossRef Medline